Journal of Applied Polymer Science

The Degradation and Charring of Flame Retarded Epoxy Resin During the Combustion

Wenchao Zhang, Xiangmei Li, Rongjie Yang
National Laboratory of Flame Retardant Materials, School of Materials, Beijing Institute of Technology, Beijing 100081, People's Republic of China
Correspondence to: R. Yang (E-mail: yrj@bit.edu.cn)

ABSTRACT: To study flame retardant mechanism of epoxy resin (EP) by octaphenyl silsesquioxane and 9,10-dihydro-9-oxa-10-phosphaphenanthrene-10-oxide, an experimental method is set up to investigate the residue of the EPs, which is extinguished during the cone calorimeter testing at different times. The chemical structures of the residues are investigated by the FTIR and XPS. The breakdown of EPs network and formation of new crosslinking structure are supported by the FTIR analysis. The changes of C and O concentrations in the condensed phase during the combustion are investigated by XPS in detail. Moreover, formation of organic carbon is uncovered by the plasmon loss curves based on XPS that could track the carbon crosslinking. These results exhibited a whole degradation and charring process of EP during the combustion: degradation of EP chain, more crosslinking charring, and thermal oxidation of the char. Furthermore, a program of combustion and degradation process of EPs is described in this research. © 2013 Wiley Periodicals, Inc. J. Appl. Polym. Sci. 130: 4119–4128, 2013

KEYWORDS: degradation; flame retardance; resins

Received 26 March 2013; accepted 19 June 2013; Published online 10 July 2013
DOI: 10.1002/app.39689

INTRODUCTION

Epoxy resins (EP) have been widely used in surface coating, adhesives, painting, and potting materials, composites, laminates, encapsulants for semiconductor, and insulating materials for electric devices because of their great versatility, toughness, low shrinkage on cure, good moisture resistance, solvent and chemical resistance, outstanding adhesion, and superior electrical and mechanical properties. However, flammability is one of the main drawback of EPs.[1–5] Traditionally, halogenated compounds have been widely used as co-monomers or additives with EPs to obtain fire-retardant materials. However, flame-retardant EPs containing bromine or chlorine can produce poisonous and corrosive smoke and may produce highly toxic halogenated dibenzodioxins and dibenzofurans.[6–8] Therefore, the development and application of halogen-free flame-retardants has been a subject of extensive investigation in relation to EPs.

In our previous work, a DOPO (9,10-dihydro-9-oxa-10-phosphaphenanthrene-10-oxide)-containing polyhedral oligomeric silsesquioxane (DOPO-POSS) was successfully synthesized.[9] An interesting phenomenon, termed the "blowing-out effect", has been detected in flame-retarded EPs with DOPO-POSS loading.[10] Moreover, the "blowing-out effect" can also take place in EPs flame-retarded by a mixture of OPS (octaphenyl silsesquioxane) and DOPO.[11] The "blowing-out effect" has been described as follows: "after the sample was ignited, it showed an unstable flame for several seconds; with the pyrolytic gaseous products jetting outward from the condensed-phase surface, the flame was extinguished; it looks as though the gas blew out the flame". A model of the blowing-out effect is shown in Figure 1. This concept reveals that the blowing-out effect is simultaneously determined by the rate of production of gases and the properties of the condensed phase.[12]

The thermal degradation behaviors and flame retardancy of EPs have been reported a lot.[13–18] However, mechanism on the blowing-out effect still needs to be researched. In this article, in order to uncover the secret of the "blowing-out effect", an effective method is used to get the residue of EP flame retarded by OPS and DOPO during combustion. By analyzing these residues, the information on degradation and charring process of EP is obtained.

EXPERIMENTAL

Materials

Diglycidyl ether of biphenol A (DGEBA, E-44, epoxy equivalent = 0.44 mol/100 g) was purchased from FeiCheng DeYuan Chemicals. The 4, 4′-diaminodiphenylsulphone (DDS) was purchased from TianJin GuangFu Fine Chemical Research Institute. DOPO was purchased from Eutec Trading

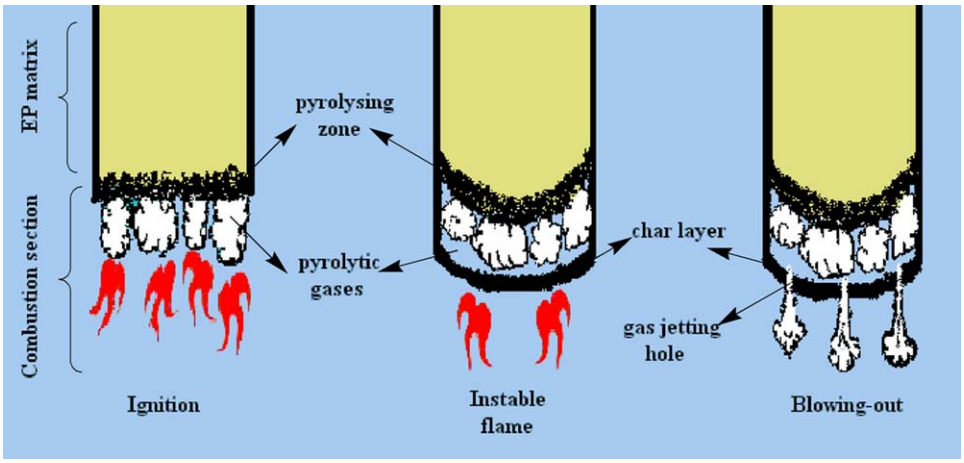

Figure 1. Model of the blowing-out effect. [Color figure can be viewed in the online issue, which is available at wileyonlinelibrary.com.]

(Shanghai). OPS was synthesized by hydrolysis and condensation of phenyltrichlorosilane according to a previously reported procedure.[19] The OPS obtained in this way had a perfect T_8 cage structure.

Preparation of the Cured EPs

The cured EPs were obtained using a thermal curing process. At first, DOPO was added to DGEBA by mechanical stirring at 140°C for 1 h, and then OPS was dispersed in the DGEBA/DOPO for a further 1 h. After that, the curing agent DDS was then added in an amount relative to DGEBA. The equivalent weight ratio of DGEBA to DDS was 9 : 2. The EPs were cured at 180°C for 4 h. The contents of OPS and DOPO in the products are listed in Table I.

Table I. Compositions of the Investigated Materials

		Content of flame retardant (wt %)			
Samples	Cured epoxy resin (wt %)	OPS	Si	DOPO	P
Pure EP	100.0	/	/	/	/
EP/DOPO/OPS	89.6	4.1	0.9	6.3	0.9

Measurements

Cone calorimeter measurements were performed according to ISO 5660 protocol at an incident radiant flux of 25 kW/m^2. The equipment is Fire Testing Technology apparatus with a truncated cone-shaped radiator. The specimen (100 × 100 × 3 mm^3) was measured horizontally without any grids. Typical results from the cone calorimeter tests were reproducible within ±10%, and the reported parameters were average value for three measurements.

To get the condensed phase residues at different times during the EP combustion, the specimen was cut into four pieces before the cone calorimeter test, and then they are recombined to a whole sample for cone test as shown in Figure 2. During the combustion of the EP in the cone testing, at different times, respectively, the four pieces were taken out, and extinguished very fast by a cover as shown in Figure 2. Then, the residue was cooled down naturally. In this way, four samples of the residues were obtained through one cone calorimeter test.

The heat release rate (HRR) curves for the pure EP and EP/DOPO/OPS are presented in Figure 3. It can be observed that the pure EP burns rapidly after ignition and HRR reaches a sharp peak with a peak HRR (p-HRR) of 635 kW/m^2. The p-HRR of EP/5%DOPO/5%OPS is 341 kW/m^2, which is much lower than that of the pure EP.

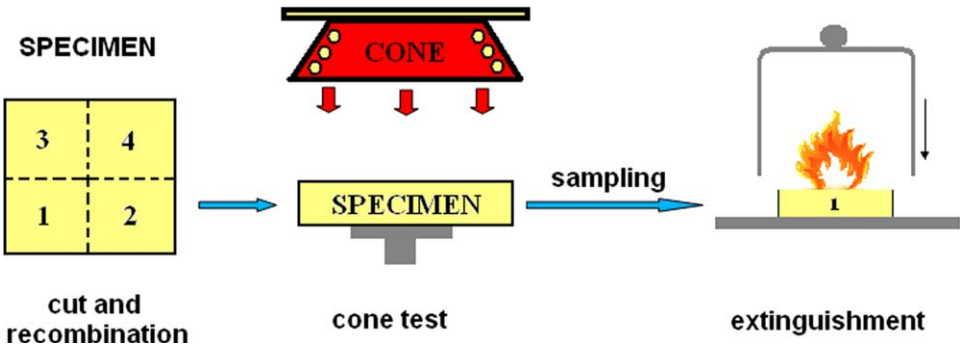

Figure 2. The sample preparation instruction. [Color figure can be viewed in the online issue, which is available at wileyonlinelibrary.com.]

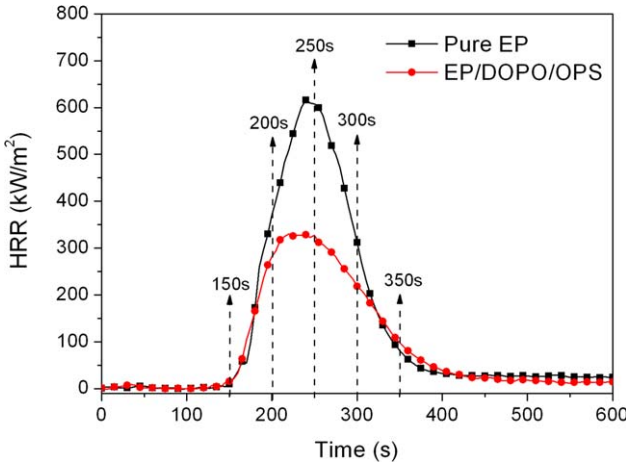

Figure 3. Heat release rate curves of pure EP and EP/DOPO/OPS. [Color figure can be viewed in the online issue, which is available at wileyonlinelibrary.com.]

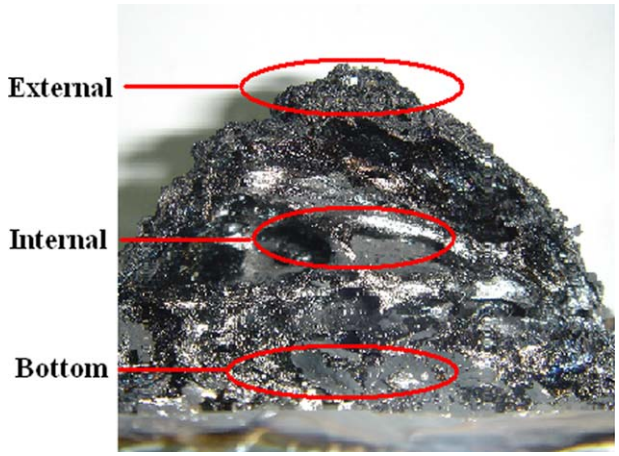

Figure 4. The positions of different residues. [Color figure can be viewed in the online issue, which is available at wileyonlinelibrary.com.]

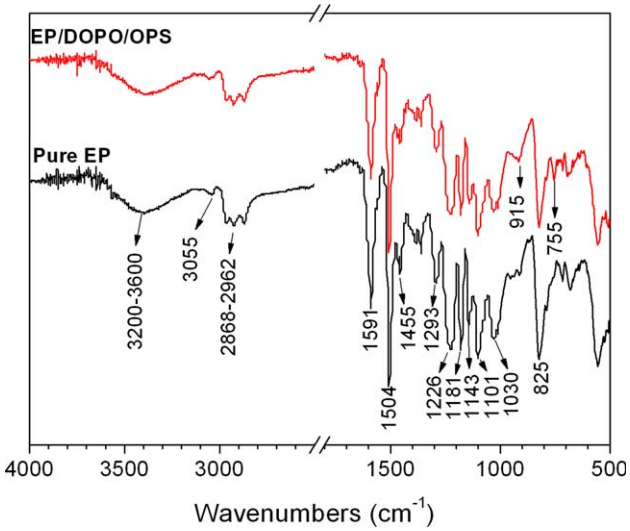

Figure 5. FTIR spectra of pure EP and EP/DOPO/OPS. [Color figure can be viewed in the online issue, which is available at wileyonlinelibrary.com.]

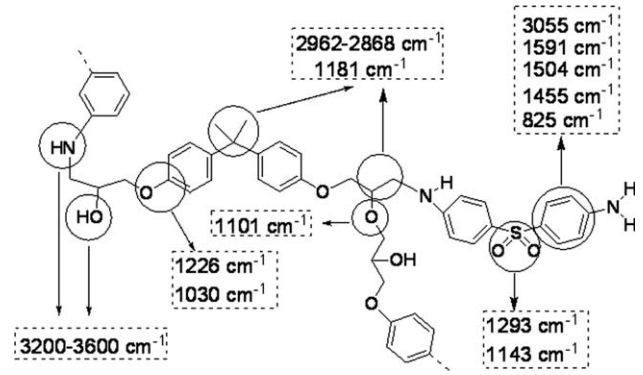

Figure 6. The origin of main absorbance bands observed in the FTIR spectra.

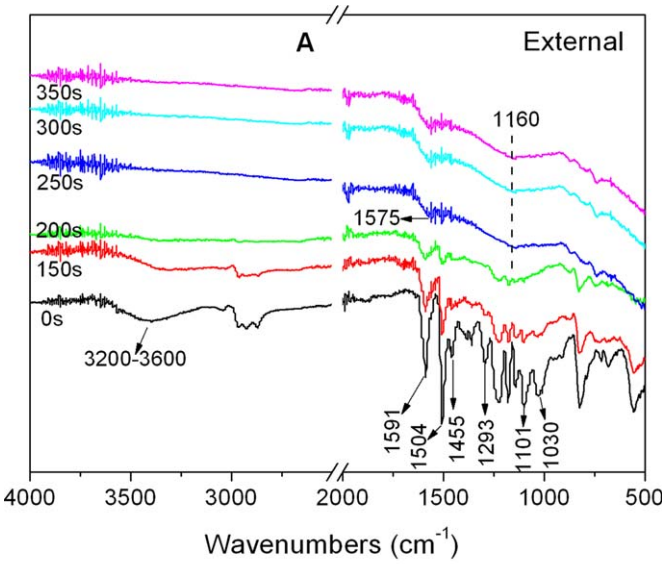

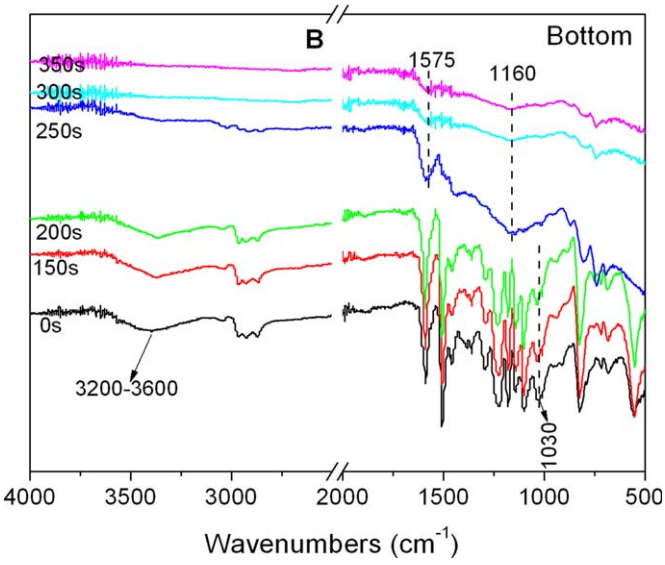

Figure 7. FTIR spectra of external and bottom residues of pure EP during the combustion. [Color figure can be viewed in the online issue, which is available at wileyonlinelibrary.com.]

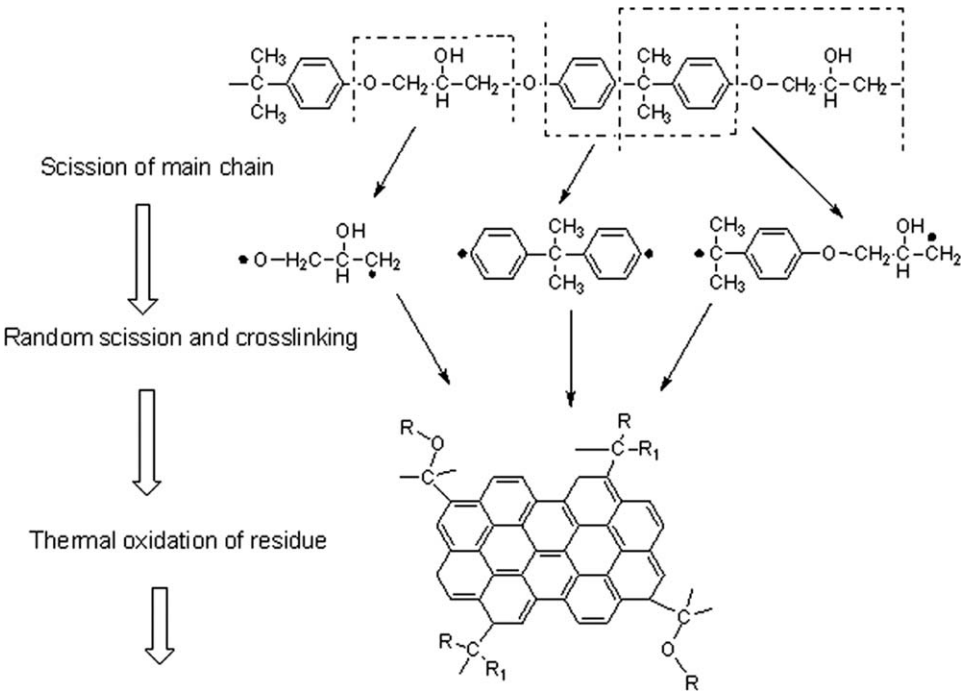

Figure 8. Main thermal degradation steps of EP matrix.

According to Figure 3, the sampling time was designed as 150, 200, 250, 300, and 350 s. To do this, the cone calorimeter test was repeated twice. In the first, the sampling time was at 150, 200, 250, and 300 s, respectively; in the second, it was 200, 250, 300, and 350 s, respectively. For every solid residue, further sampling was achieved at three local positions (external, internal, and bottom) as shown in Figure 4. For residues of the pure EP, further sampling was only at the external and bottom.

All the samples of solid residue were ground carefully. Then, they were analyzed by FTIR (Nicolet 6700) in ATR mode and by X-ray photoelectron spectroscopy (XPS) measurements (Ulvac-PHI) at 25 W and 15 kV under a vacuum better than 10^{-6} Pa. In XPS analysis, the sample was neutralized by both an ion-gun and an electronic-gun. To compensate for sample charging all binding energies were referenced to C1s at 284.9 eV. A variation in the position of each peak of ±0.1 eV was considered acceptable.

RESULTS AND DISCUSSION

FTIR Analysis on the Degradation and Charring of EP Composites

FTIR spectra of pure EP and EP/DOPO/OPS are shown in Figure 5. It can be seen that peaks at 3200–3600, 3055, 2868–2962, 1591, 1504, 1455, 1293, 1226, 1181, 1143, 1101, 1030, and 825 cm^{-1} are the characteristic absorbance of EP networks.[1,2,20] The chemical bonds corresponding to the absorbance are outlined in Figure 6. Moreover, the P-O-phenyl stretching vibration at 915 cm^{-1} and the C-H deformation vibration of phenyl rings of DOPO groups at 755 cm^{-1} from DOPO-POSS are identified.[20,21]

Analysis for Solid Residue from Pure EP. FTIR spectra of external residue of pure EP at different times are shown in Figure 7(A). For the external residue corresponding ignition time (150 s), the main characteristic absorbance of EP network remain, nevertheless, an evident decrease of absorbance of C-O and -O- at 1101 and 1030 cm^{-1} can be observed, which indicates that the scission of C-O occurring in the early step of thermal degradation of the epoxy network.[2,20] Similar degradation for the O=S=O bond in DDS at 1293 cm^{-1} also happens in this early step.[1] These results mean that the initial combustion is caused by the ignition of flammable volatile fragment created by the scission of EP chains in the surface zone. In the external residue at 200 s, the significant changes of the epoxy network are observed. The absorbance of -OH and -NH bonds (3200–3600 cm^{-1}) disappear totally. The aliphatic components (2962–2868 and 1181 cm^{-1}), aromatic ring C=C stretching vibration (1591, 1504, and 1455 cm^{-1}), alkyl-aryl ether bonds (1226 and 1030 cm^{-1}), and alkyl ether bonds (1101 cm^{-1}) decrease remarkably. These indicate that the molecular structures of EP are destroyed seriously. In the residue at 250 s, the absorbance of aliphatic components disappears totally, the aromatic ring C=C stretching vibration at 1591 and 1504 cm^{-1} disappear, and a new broader absorbance at 1575 cm^{-1} appears, indicating the formation of polyaromatic carbons by crosslinking.[11] Moreover, the broad absorbance at 1160 cm^{-1} indicates the formation of C-O bond by thermal oxidation of polyaromatic carbons.[11] For the residue at 300 and 350 s, their FTIR spectra are similar to that at 250 s, indicating the chemical structure of residue after 250 s became stable with consumption of this residue through the thermal oxidation process.

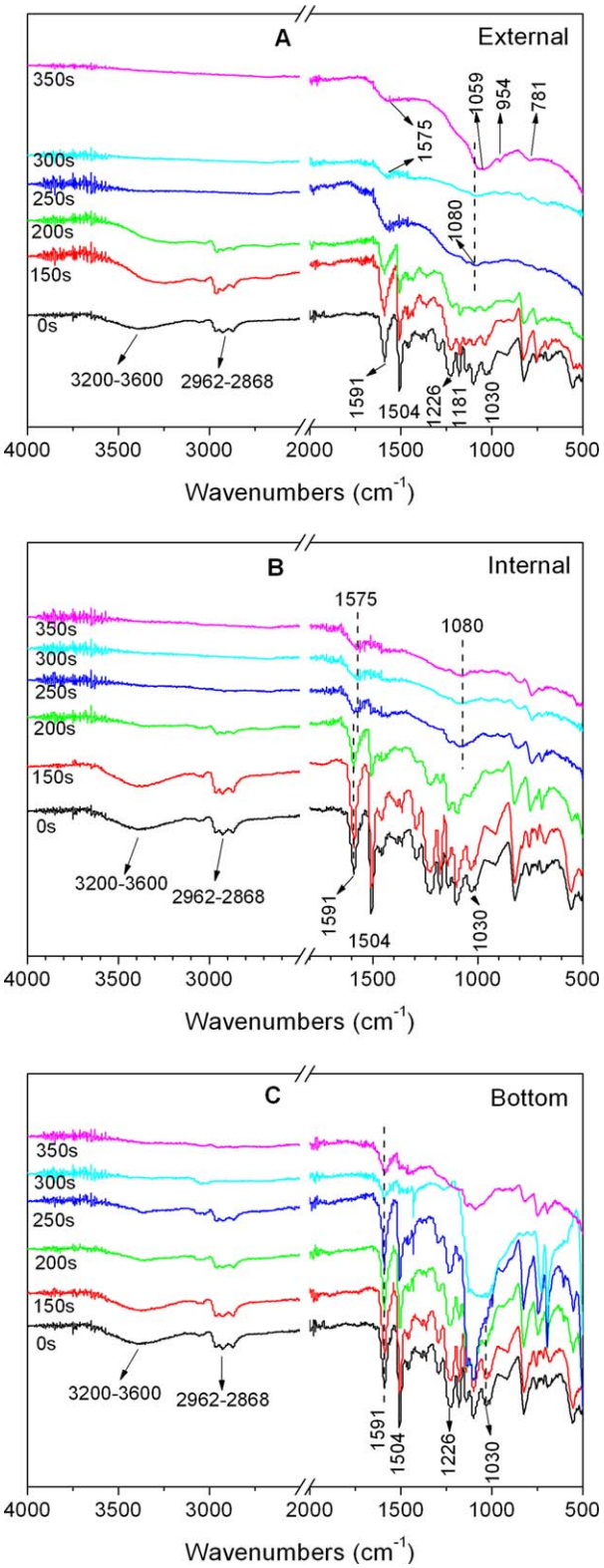

Figure 9. FTIR spectra of external, internal, and bottom residues of EP/DOPO/OPS during the combustion. [Color figure can be viewed in the online issue, which is available at wileyonlinelibrary.com.]

FTIR spectra of bottom residues of pure EPs are shown in Figure 7(B). For the residue at 150 and 200 s, their chemical structures are similar to that of 0 s, there are only little shift and decrease of absorbance of N-H and O-H at 3200–3600 cm^{-1} can be observed. Furthermore, the diminishing absorbance of C-O at 1030 cm^{-1} from 0 to 200 s samples also can be detected. This means the scission of a few of C-O bonds in EP happen in the early stage. In the residue at 250 s, the absorbance of -OH and -NH related bonds disappear totally. The aliphatic components, aromatic ring C=C stretching vibration, alkyl-aryl ether bonds, and alkyl ether bonds decrease remarkably. These changes in bottom residue are almost similar to the external residue at 200 s in Figure 7(A). In the bottom residue at 300 and 350 s, the polyaromatic carbon at 1575 cm^{-1} is detected. Thermal degradation of the EP at bottom is a little later than that of the external EP.

Table II. Element Concentration of the Residues of Pure EP by XPS (%)

	External		Bottom	
Sample	C	O	C	O
0 s	80.58	17.00	80.58	17.00
150 s	84.83	11.64	83.86	13.35
200 s	86.10	9.88	83.85	12.40
250 s	89.61	6.96	86.97	9.93
300 s	86.93	11.28	90.06	6.63
350 s	84.08	13.34	86.17	10.48

The thermal degradation process of the EP is shown in Figure 8, including scission of main chain, random scission, crosslinking, and thermal oxidation.

Analysis for *Solid Residue* from EP/DOPO/OPS. The spectra of external residue of EP/DOPO/OPS samples are shown in Figure 9(A). From 0 s sample to 250 s sample, the absorbance of -OH and -NH related bonds (3200–3600 cm^{-1}), the aliphatic components (2962–2868 and 1181 cm^{-1}), aromatic ring C=C stretching vibration (1591, 1504, and 1455 cm^{-1}), alkyl-aryl ether bonds (1226 and 1030 cm^{-1}), and alkyl ether bonds (1101 cm^{-1}) decrease remarkably. Moreover, the polyaromatic carbon at 1575 cm^{-1} is detected for the 250 and 300 s sample. For the 350 s sample, some dramatic changes are detected in Figure 9(A). The C=C stretching vibration of polyaromatic carbons at 1575 cm^{-1} is clearly enhanced and some C_{Ar}-H deformation vibration could be detected at 781 cm^{-1}. In addition,

Table III. Element Concentration of the Residues of EP/DOPO/OPS by XPS (%)

	External		Internal		Bottom	
Sample	C	O	C	O	C	O
0 s	78.63	17.55	78.63	17.55	78.63	17.55
150 s	84.22	11.55	82.87	11.71	79.18	15.01
200 s	85.13	10.46	82.80	11.34	76.55	14.83
250 s	85.93	10.00	82.62	12.17	77.30	15.66
300 s	86.20	9.19	82.57	12.27	77.80	15.41
350 s	83.20	11.40	83.80	11.80	78.28	15.11

Table IV. Plasmon Loss Data for the Pure EP

	External			Bottom		
Sample	C1s (eV)	C1s Plasmon (eV)	C1s $\triangle EL$ (eV)	C1s (eV)	C1s Plasmon (eV)	C1s $\triangle EL$ (eV)
0 s	284.9	308.0	23.1	284.9	308.0	23.1
150 s	284.9	308.3	23.4	284.9	308.5	23.6
200 s	284.9	308.8	23.9	284.9	308.5	23.6
250 s	284.9	310.8	25.9	284.9	309.2	24.3
300 s	284.9	311.0	26.1	284.9	310.2	25.3
350 s	284.9	311.2	26.3	284.9	311.4	26.5

the new broad absorbance at 1059 cm^{-1} becomes apparent, which means more C-O and Si-O structures exist in the residue. Another new absorbance peak at 954 cm^{-1}, which represents the Si-O-phenyl and P-O-phenyl stretching vibrations, is detected.[20,22]

The internal residues of EP/DOPO/OPS are shown in Figure 9(B). During the combustion, its thermal degradation process is similar but later than in external residue of EP/DOPO/OPS. The absorbance for Si-O, Si-O-phenyl, and P-O-phenyl do not appear in the internal residue at 350 s.

The spectra of bottom residue of EP/DOPO/OPS are shown in Figure 9(C). The thermal degradation of bottom EP matrix is apparently late. The main chemical structures of EP such as -OH and -NH related bonds (3200–3600 cm^{-1}), the aliphatic components (2962–2868 and 1181 cm^{-1}), aromatic ring C=C stretching vibration (1591, 1504, and 1455 cm^{-1}), alkyl-aryl ether bonds (1226 cm^{-1}) are kept until 250 s; moreover, the crosslinking structure of polyaromatic carbons at 1575 cm^{-1} cannot be detected in the 350 s sample.

It can be easily find that the EP matrix of EP/DOPO/OPS undergoes similar thermal degradation process to the pure EP as shown in Figures 8 and 9. Because of the existence of DOPO/OPS, the formation of Si-O, Si-O-phenyl and P-O-phenyl structure that can enhance the thermal stability of char layer can be detected in the external residue of EP/DOPO/OPS. Addition of DOPO/OPS slows down thermal degradation of EP matrix in the bottom.

XPS Analysis on Residues of EP Composites

Analysis for *Solid Residue* from *Pure* EP. The C and O concentrations in the residue obtained for the pure EP and EP/DOPO/OPS are shown in Tables II and III. The plasmon loss ($\triangle E_L$)[23–26] is defined as the difference between the main peak in C1s spectra and the plasmon peak in C1s spectra. The plasmon loss data of pure EP and EP/DOPO/OPS are summarized in Tables IV and V.

Figure 10(A) shows the C concentration in external and bottom residues of pure EP as a function of combustion time. It should be noted that the C concentration increase gradually for external residue from 0 to 250 s and for bottom residue from 0 to 300 s. The early increase of the C concentration of implies that the other elements, probably hydrogen-rich fragments, are losing from the surface with crosslinking processes in condensed phase caused by the interaction between radical fragments.[23–26] As shown in Figure 10(A), from 0 to 250 s, the C concentration in the bottom residue are lower than that in the external residue, which indicates the crosslinking reaction in the bottom are later than that in the external.[23–26]

At 250 and 300 s for the external and bottom residues, respectively, the C concentration reaches the maximum, later it starts to decrease. This correlates with thermal oxidation in condensed phase.

Change of the O concentrations with time in residues of the pure EP is contrary to that of the C concentration shown in Figure 10(B). The reduction of oxygen corresponds to

Table V. Plasmon Loss Data for the EP/DOPO/OPS

	External			Internal			Bottom		
Sample	C1s (eV)	C1s Plasmon (eV)	C1s $\triangle E_L$ (eV)	C1s (eV)	C1s Plasmon (eV)	C1s $\triangle E_L$ (eV)	C1s (eV)	C1s Plasmon (eV)	C1s $\triangle EL$ (eV)
0 s	284.9	307.7	22.8	284.9	307.7	22.8	284.9	307.7	22.8
150 s	284.9	308.5	23.6	284.9	308.3	23.4	284.9	308.2	23.3
200 s	284.9	309.5	24.6	284.9	308.6	23.7	284.9	308.4	23.5
250 s	284.9	310.9	26.0	284.9	309.6	24.7	284.9	308.5	23.6
300 s	284.9	311.0	26.1	284.9	309.9	25.0	284.9	308.7	23.8
350 s	284.9	311.1	26.2	284.9	310.2	25.3	284.9	308.9	24.0

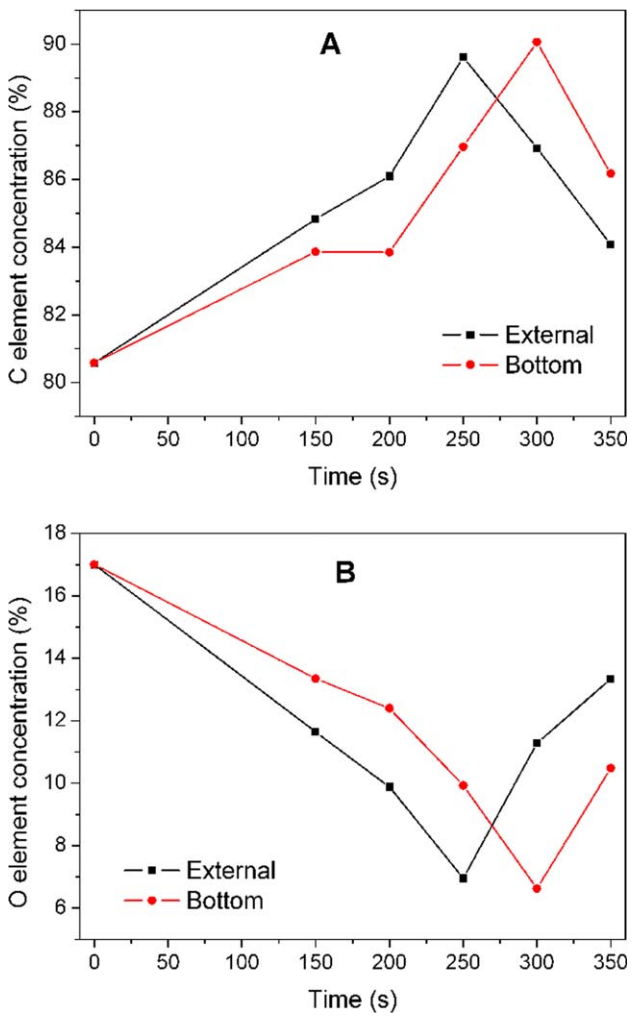

Figure 10. Dynamic change of C and O concentration in external and bottom residues of pure EP as a function of combustion time. [Color figure can be viewed in the online issue, which is available at wileyonlinelibrary.com.]

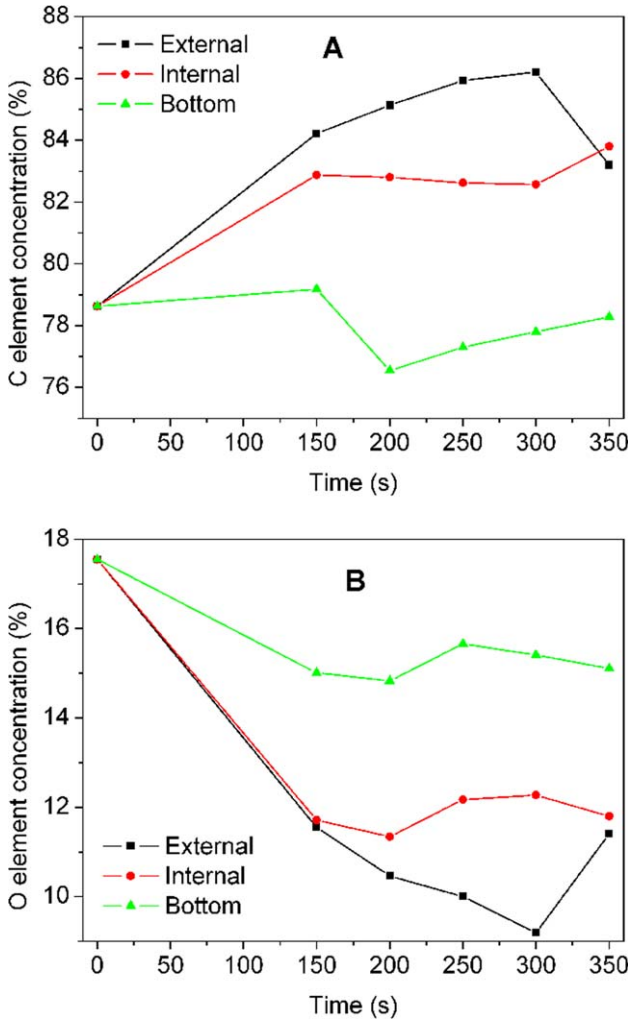

Figure 12. Dynamic change of C and O concentration in external, internal, and bottom residues of EP/DOPO/OPS as a function of combustion time. [Color figure can be viewed in the online issue, which is available at wileyonlinelibrary.com.]

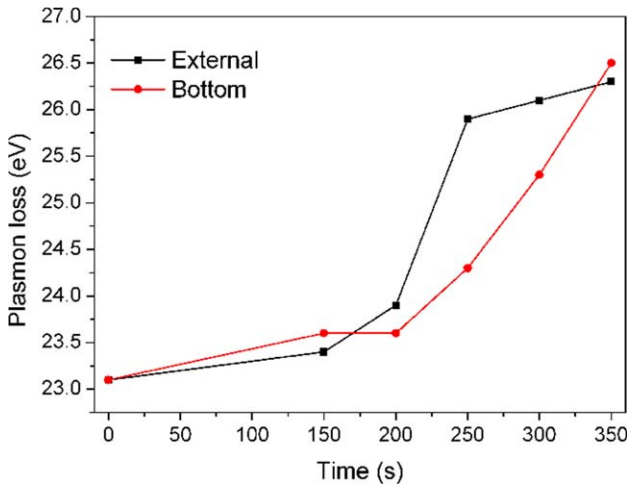

Figure 11. Plasmon loss as function of combustion time for pure EP. [Color figure can be viewed in the online issue, which is available at wileyonlinelibrary.com.]

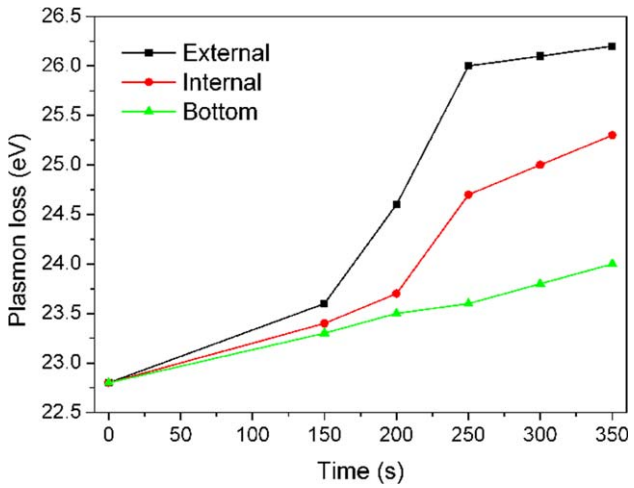

Figure 13. Plasmon loss as function of combustion time for EP/DOPO/OPS. [Color figure can be viewed in the online issue, which is available at wileyonlinelibrary.com.]

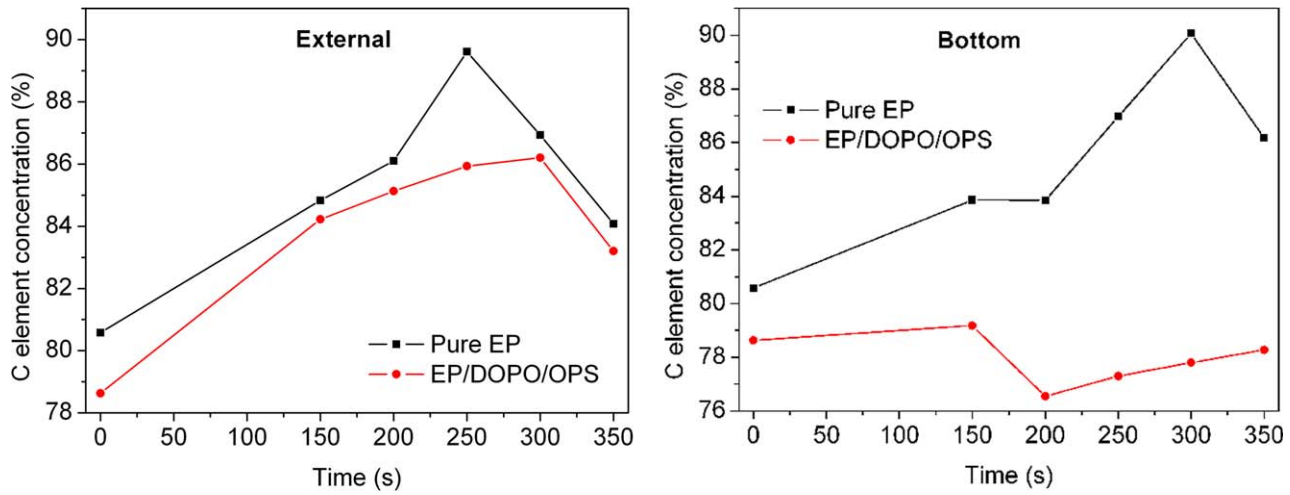

Figure 14. Comparison of C concentration of external and bottom residues for pure EP and EP/DOPO/OPS. [Color figure can be viewed in the online issue, which is available at wileyonlinelibrary.com.]

degradation reactions of the EP network structure through scission of C-O and -O- bonds with releasing volatile fragments until the minimum O concentration. After that, thermal oxidation of the condensed phase C becomes dominant, which leads to the accumulation of oxygen in the residue.

The process of degradation and charring can be examined by exploring the formation of organic carbon by the plasmon loss curves of carbon as a function of time as shown in Figure 11. An increase of the plasmon loss value is correlated with the extent of organization of carbon, and hence with crosslinking.[23–26] We can clearly see that this parameter increases slowly from 0 to 200 s, rapidly from 200 to 250 s for external residue and from 200 to 350 s for the bottom residue, which means early a little, and late large amount, crosslinking among polymer chains through radicals recombining. For the external residue after 250 s, the plasmon loss value increases very slowly. This may be because of that thermal oxidation is dominant after 250 s.

Analysis for Solid Residue from EP/DOPO/OPS. Figure 12(A) shows the C concentration in external, internal, and bottom residues of EP/DOPO/OPS as a function of combustion time. It should be noted that the C concentration in the external residue increases quickly from 0 to 300 s, and then shows a rapid decrease after 300 s. The increase of carbon indicates the rapid crosslinking processes, and its decrease does thermal oxidation in the condensed phase. It seems that for the EP/DOPO/OPS, the C concentration keeps constant basically in long time (150–300 s) according to Figure12(A), which means stable C crosslinking structure in the condensed phase. This could explain well the reason of the low p-HRR of EP/DOPO/OPS (Figure 3).

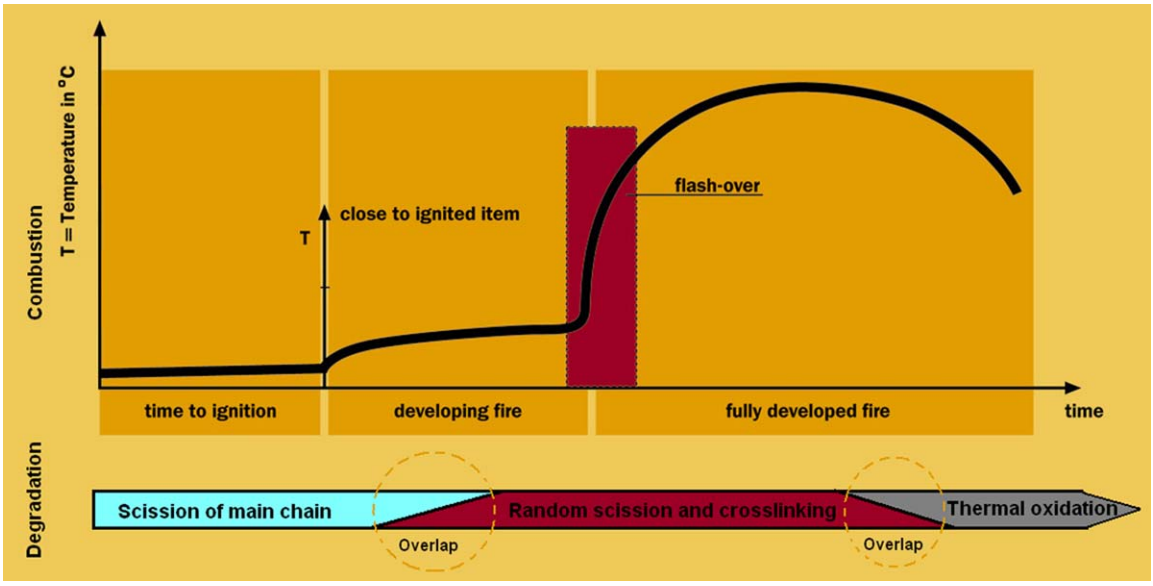

Figure 15. Simulation program of combustion and degradation process of EPs as a function of time. [Color figure can be viewed in the online issue, which is available at wileyonlinelibrary.com.]

For the bottom residue, the C concentration decreases at 200 s. This is caused by the increase of Si element at the bottom because of the subsidence of OPS at the early stage of thermal degradation process.

Change of O concentrations in the external residue [Figure 12(B)] is contrary to that of C concentration because of the rapid crosslinking processes in the beginning and thermal oxidation later in the condensed phase.

In addition, it is noted that in the bottom residue, the O and C concentrations are much higher, or lower, than that those in external residue, respectively. These may indicate that the EP matrix in the bottom maintains stable because of insulation of the more char above it.

In Figure 13, the plasmon loss values increase with time for the external, internal, and bottom residues, which means an enhanced extent of organization of carbon caused by crosslinking. Furthermore, it is also noted that the external, internal, and bottom residues have the maximum, middle, and minimum plasmon loss values, respectively, meaning high, moderate, and weak crosslinking in them.

Comparison of XPS Analysis for Pure EP and EP/DOPO/OPS. As shown in Figure 14, the addition of DOPO/OPS causes a remarkable difference in C concentrations of residue in pure EP and EP/DOPO/OPS. In the external residue, the C concentration for pure EP is a little higher than for EP/DOPO/OPS; in the bottom residue, the C concentration for pure EP is much higher than for EP/DOPO/OPS. This may imply high thermal stability of the EP/DOPO/OPS because of existence of Si-O, Si-O-phenyl, and P-O-phenyl structure in the residue.

Discussion about the Combustion of Pure EP and EP/DOPO/OPS

According to analysis on the residues at different time for the pure EP and EP/DOPO/OPS, we can conclude that the ignition is caused by flammable volatile fragments from the scission of the EP chain in surface, then, the internal EP matrix begins to decompose and feeds the gaseous product to the surface to support the combustion, with formation of the crosslinking structure from the external to bottom. With acceleration of thermal degradation of the EP matrix, rich combustible fuel feed leads to the flashover. After it the thermal oxidation degradation of the char layer becomes a dominant process. The program of combustion and degradation process of the EPs with time is shown in Figure 15.

For the EP/DOPO/OPS, the existence of Si-O, Si-O-phenyl, and P-O-phenyl structures in the external charring could enhance the thermal stability of the char layer, and supply a better protection to the EP matrix below it.

CONCLUSIONS

Through cutting the specimen for the cone calorimeter test into four pieces, and sampling one piece at different time one time, we set up an experimental method to study char structure during combustion of the EP flame retarded by OPS and DOPO. Through analyzing the residues at different combustion time by FTIR and XPS, we find the changes of chemical structures in the external, internal, and bottom residues.

The FTIR and XPS analysis on these residues indicate that the ignition of EP is caused by flammable volatile fragments because of the scission of the EP chain in surface. Then, the fast internal degradation and combustible gas release lead to the flashover with charring, and the C element begins to increase because of fast crosslinking reaction. Finally, the thermal oxidation degradation in the char layer becomes a dominant process. The DOPO/OPS as flame retardants are helpful to enhance the thermal stability of external char layer. This char layer can inhibit the degradation and gaseous products release of the EP matrix.

ACKNOWLEDGMENT

This work was funded by National Natural Science Foundation of China (No. 51273023).

REFERENCES

1. Schartel, B.; Balabanovich, A. I.; Braun, U.; Knoll, U.; Artner, J.; Ciesielski, M.; Döring, M.; Perez, R.; Sandler, J. K. W.; Altstädt, V.; Hoffmann, T.; Pospiech, D. *J. Appl. Polym. Sci.* **2007**, *104*, 2260.
2. Wang, X.; Hu, Y.; Song, L.; Xing, W. Y.; Lu, H. D.; Lv, P.; Jie, G.X. *Polymer* **2010**, *51*, 2435.
3. Liu, H.Z.; Zheng, S. X.; Nie, K. M. *Macromolecules* **2005**, *38*, 5088.
4. Brus, J.; Urbanová, M.; Strachota, A. *Macromolecules* **2008**, *41*, 372.
5. Liu, R.; Wang, X.D. *Polym. Degrad. Stab.* **2009**, *94*, 617.
6. Wang, J. -S.; Liu, Y.; Zhao, H. -B.; Liu, J.; Wang, D. -Y.; Song, Y. -P.; Wang, Y. -Z. *Polym. Degrad. Stab.* **2009**, *94*, 625.
7. Chow, W. S.; Neoh, S. S. *J. Appl. Polym. Sci.* **2009**, *114*, 3967.
8. Becker, L.; Lenoir, D.; Matuschek, G.; Kettrup, A. *J. Anal. Appl. Pyrolysis* **2001**, *60*, 55.
9. Zhang, W. C.; Yang, R. J. *J. Appl. Polym. Sci.* **2011**, *122*, 3383.
10. Zhang, W. C.; Li, X. M.; Yang, R. *J. Polym. Degrad. Stab.* **2011**, *96*, 2167.
11. Zhang, W. C.; Li, X. M.; Li, L. M.; Yang, R. *J. Polym. Degrad. Stab.* **2012**, *97*, 1041.
12. Zhang, W. C.; Li, X. M.; Yang, R. *J. Polym. Degrad. Stab.* **2012**, *97*, 1314.
13. Yu, D.; Kleemeier, M.; Wu, G. M.; Schartel, B.; Liu, W. Q.; Hartwig, A. *Macromol. Mater. Eng.* **2011**, *296*, 952.
14. Schartel, B.; Braun, U.; Balabanovich, A. I.; Artner, J.; Ciesielski, M.; Döring, M.; Perez, R. M.; Sandler, J. K. W.; Altstädt, V. *Eur. Polym. J.* **2008**, *44*, 704.
15. Perret, B.; Schartel, B.; Stoss, K.; Ciesielski, M.; Diederichs, J.; Doring, M.; Krömer, J.; Altstädt, V. *Eur. Polym. J.* **2011**, *47*, 1081.
16. Wang, Z. F.; Liu, W. Q.; Hu, C. H.; Ma, S. Q. *J. Appl. Polym. Sci.* **2011**, *121*, 2213.

17. Spontón, M.; Mercado, L. A.; Ronda, J. C.; Galià, M.; Cádiz, V. *Polym. Degrad. Stab.* **2008**, *93*, 2025.
18. Zhang, W. C.; Li, X. M.; Fan, H. B.; Yang, R. *J. Polym. Degrad. Stab.* **2012**, *97*, 2241.
19. Li, L. M.; Li, X. M.; Yang, R. J. *J. Appl. Polym. Sci.* **2011**.DOI 10.1002/app.35443.
20. Zhang, W. C.; Li, X. M.; Yang, R. *J. Polym. Degrad. Stab.* **2011**, *96*, 1821.
21. Zhang, W. C.; Li, X. M.; Guo, X. Y.; Yang, R. *J. Polym. Degrad. Stab.* **2010**, *95*, 2541.
22. Lin, H. T.; Lin, C. H.; Hu, Y. M.; Su, W. C. *Polymer* **2009**, *50*, 5685.
23. Du, J. X.; Zhu, L.; Wilkie, C. A.; Wang, J. Q. *Polym. Degrad. Stab.* **2002**, *77*, 377.
24. Hao, J. W.; Wilkie, C. A.; Wang, J. Q. *Polym. Degrad. Stab.* **2001**, *71*, 305.
25. Du, J. X.; Wang, D. Y.; Wilkie, C. A.; Wang, J. Q. *Polym. Degrad. Stab.* **2003**, *79*, 319.
26. Wang, J. Q.; Li, B. *Polym. Degrad. Stab.* **1999**, *63*, 279.